COBEM 2021 26th International Congress of Mechanical Engineering
November 22-26, 2021, Virtual Congress, Brazil

COB-2021-0632
THERMAL EFFICIENCY OF OPEN-CELL METAL FOAMS WITH DIFFERENT THICKNESS: A COMPARATIVE ANALYSIS BETWEEN CORRELATIONS AND NUMERICAL MODELING

Leonardo Lachi Manetti[1,2]
leonardo.manetti@ifms.edu.br
[1]IFMS - Federal Institute of Education, Science and Technology of Mato Grosso do Sul, Campus Campo Grande, Campo Grande, MS, Brazil.
Iago Lessa de Oliveira[2]
iago.oliveira@unesp.br
Elaine Maria Cardoso[2,3*]
*elaine.cardoso@unesp.br, corresponding author
[2]UNESP – São Paulo State University, School of Engineering, Graduate Program in Mechanical Engineering, Av. Brasil, 56, 15385-000, Ilha Solteira, SP, Brazil.
[3]UNESP – São Paulo State University, Campus of São João da Boa Vista, São João da Boa Vista, SP, Brazil

Abstract. *This work used numerical techniques to calculate the extended surface efficiency and analyze the impact of the foam's thickness on its efficiency. Heat conduction was simulated in open-cell copper foam with three different thicknesses, 3 mm, 2 mm, and 1 mm, under convection boundary conditions obtained from pool boiling experiments with two dielectric fluids, HFE-7100 and Ethanol, at saturation conditions and atmospheric pressure. The geometries of the foams were segmented from μCT images, converted to the stereolithography (STL) format, and used to build the computational meshes. The numerical simulations were carried out in foam-extend-4.0. The numerical extended surface efficiency was compared with classical analytical models and other correlations from the literature. The foam efficiency increased as the thickness decreased. The thinnest copper foam showed better efficiency than the other ones. Metal foam under pool boiling of Ethanol had lower efficiency than HFE-7100. The pin fin model with adiabatic tip presented the lowest mean absolute error, lower than 10% for all cases, being the copper foam with 1 mm and HFE-7100 the case with the lowest error, approximately 1%. On the other hand, the models that consider a three-dimensional matrix presented errors higher than 30%.*

Keywords: *thermal efficiency, metal foam, numerical analysis, foam thickness, convective boiling*

1. INTRODUCTION

Direct-immersion cooling with two-phase change can increase power density and energy efficiency in electronic cooling (Chen et al., 2020; Fan and Duan, 2020). The dielectric liquid cooling used to avoid a short-circuit has relatively poor thermophysical properties and an extremely small contact angle, requiring a large superheat to initiate the boiling process (Liang and Mudawar, 2019)

Heat transfer in immersion cooling begins with natural convection at low differences in the surface temperature. With further increase of the heater surface superheat, nucleate boiling starts up to the critical heat flux (CHF). The operating temperature of electronic devices should be below this superheat value to prevent CHF (Chen et al., 2020). In addition, reports show that the electronic temperature must be lower than 85 °C (El-Genk, 2012; Liang and Mudawar, 2019). Therefore, the use of an engineered surface has been studied to meet the cooling requirements of modern electronic devices (Abreu et al., 2018; Kiyomura et al., 2020).

Porous structures like the open-cell metal foams were tested by Manetti et al. (2020a, 2020b), which found that: (i) metal foam surfaces provided a higher heat transfer coefficient (HTC) compared to plain surfaces and prevented thermal overshoot at the onset nucleate boiling; (ii) there is no constant value for optimum foam thickness, *i.e.*, the optimum foam thickness varies with the heat flux; and (iii) the foam thermal conductivity plays a role in foam-finned efficiency.

Some authors tried simplifying models of the heat conduction in metal foams to obtain the foam-finned efficiency. Dukhan et al. (2005) presented a one-dimensional heat transfer model for open-cell metal foams, assuming the geometry of the solid ligaments as a bank of cylinders (pin fin). Ghosh (2008) modeled forced-convection heat transfer in an open-cell metal foam attached to an isothermal surface, assuming the foam matrix as a repetitive cubic structure. He considered the forced-convective heat transfer coupled with heat conduction through the foam fibers. Analytical expressions have been derived for the gas-solid temperature difference, the total heat transfer through the foam, and the efficiency of the foam as an extended surface in analogy with the traditional fin theory. Mancin et al. (2013, 2010)

developed a simplified scheme for overall foam-finned surface efficiency, which considered the metal foam specific area and an equivalent length proposed by the authors.

The study of heat transfer in metal foams via computational techniques is scarce, as reported by Khaled (2017). In this work, numerical simulations were carried out to calculate the metal foam-finned efficiency and compare it with available analytical/empirical models for different thicknesses of the metal foams.

2. NUMERICAL METHODOLOGY

2.1 Foam geometries

A metal foam of copper (Cu foam) with an open structure and original thickness of approximately 3 mm was used to obtain the geometries for the numerical simulations. First, μCT images were taken from the 3 mm thickness foam using a Skyscan 1272 at a resolution of 15 μm (100 kV X-ray source voltage). Second, the foams' images were segmented using the VMTK® library and converted to the stereolithography (STL) format. Finally, we sectioned the segmented geometries to one-eighth of their original size to reduce the simulation computational cost (as shown in Figure 1a) and cut them to obtain two geometries with 2 mm and 1 mm in thickness, as shown in Figure 1b (each new geometry is indicated and illustrated with different opacities). This approach is reasonable since the foams' structure is homogeneous and the procedure followed closely the one performed by Manetti et al. (2020b) in their experiments.

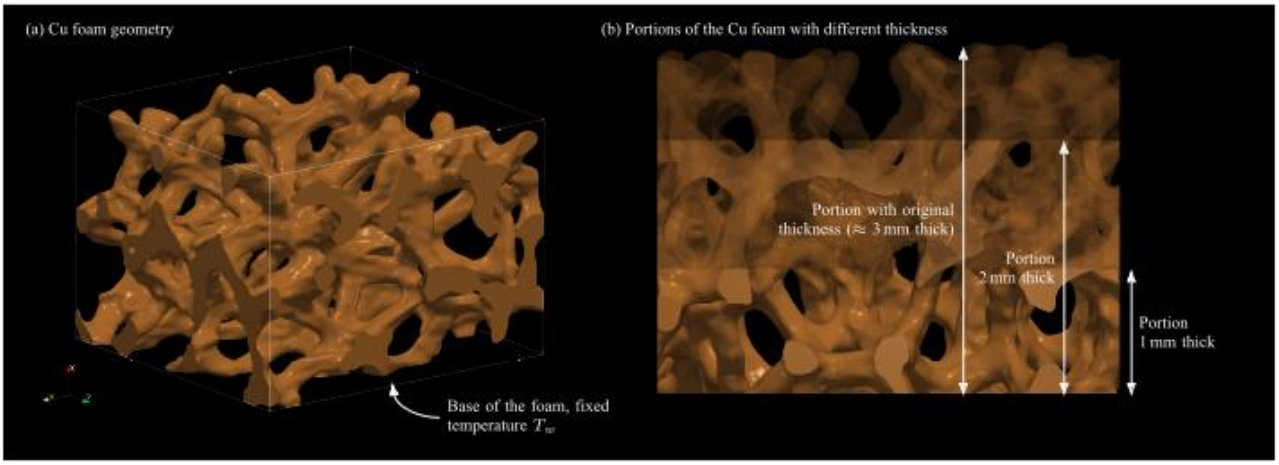

Figure 1. (a) Cu foam geometry indicating the base where a fixed temperature of T_w was applied for the numerical simulations; and (b) indication of different thicknesses used in the numerical analysis.

The μCT images were also used to characterize the foam granulometry (cell, porous, and fiber diameters) using iMorph software, as reported by Manetti et al. (2021). Table 1 shows the main characteristics of Cu foam.

Table 1. Metals foams characteristics from Manetti et al. (2021).

Foam	PPI[a] [in^{-1}]	ε [%]	d_p [mm]	d_f [mm]
Cu	31.75	90.0	0.46	0.13

[a]Pores Per Inch

2.2 Computational Meshes and Numerical Strategies

We used the foam-extend library, version 4.0, to build the computational meshes and carry out the numerical simulations. This library implements the Finite Volume Method (FVM) for the discretization and solution of partial differential equations, which guarantees second-order accuracy. The steady-state 3D conduction equation was solved for the temperature until its convergence with a normalized residual tolerance of 1×10^{-12}. The second-order accurate central differences scheme, with non-orthogonal correction, was used to discretize the Laplacian term of the conduction equation (Jasak, 1996).

The computational meshes were created using the utility "cartesianMesh" of foam-extend (within the library cfMesh), which automatically builds polyhedral hexahedral-dominant meshes for better accuracy discretization. The computational meshes of the Cu foam for each thickness, as shown in Figure 1a, had approximately 1 to 4 million cells to ensure a mesh-independent solution. The mesh-independence test was performed with the geometry of 3 mm thickness by constructing three systematically refined meshes: a coarse, an intermediate, and a fine mesh with approximately 600k, 3.5 million, and 4.5 million cells and comparing the temperature fields and the resulting heat

transfer rate calculated for each mesh. Qualitatively, the temperature distributions among the meshes did not exhibit visible differences. Quantitatively, the heat transfer rate exhibited changes of less than 1% between the two finer meshes. We considered the finer mesh with 4 million cells and cell density of approximately 500k cells/mm^3 because the computational time did not increase substantially between the three meshes; furthermore, the finer mesh assured the use of cells small enough to capture the foam surface curvature. This procedure was suitable for this work because the numerical simulation only considered heat conduction in a solid. Subsequently, the cells density found was used to define a suitable mesh for the geometry of the other thicknesses. Figure 2 shows a portion of the Cu foam mesh with 3 mm (indicated in green in the thumbnail at the top left corner) with a detail of the mesh structure obtained in foam-extend.

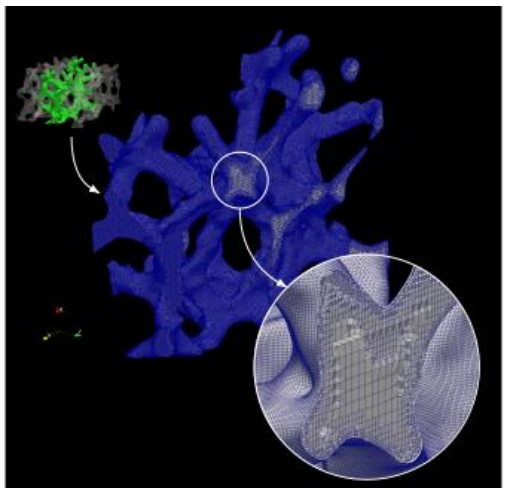

Figure 2. Details of the Cu foam geometry (green part in the thumbnail at the top left corner) showing the mesh's hexahedral-dominant structure.

2.3 Boundary conditions

The conduction problem's boundary conditions (BCs) were: fixed temperature on the base of the foam, T_w, (indicated in Figure 1a) and convective condition on the foam's surface. Both the wall temperature, T_w, and the heat transfer coefficient, h_{exp}, used in the convective BC were obtained from Manetti et al. (2021), where pool boiling experiments with two dielectric fluids, HFE-7100 and Ethanol, at saturation conditions and atmospheric pressure were carried out. For each thickness, both fluids were tested. Four cases for each surface-fluid combination were selected based on the heat fluxes: A. low, B. low-medium, C. medium, and D. high heat flux. Table 2 shows the BCs of the simulated cases.

Table 2. Boundary conditions for metal foam with 3 mm in thickness from Manetti et al. (2021).

Foam thickness	Fluid	Case	T_w [K]	h_{exp} [kW/m^2·K]	q'' [kW/m^2]
3 mm	HFE-7100[a]	A	337.36	4.87	20.44
		B	339.51	7.16	45.78
		C	345.99	11.32	146.02
		D	357.21	12.34	294.80
	Ethanol[b]	A	356.86	9.54	56.31
		B	358.14	14.49	104.47
		C	361.05	24.48	244.46
		D	364.50	27.39	367.98
2 mm	HFE-7100	A	337.11	5.19	20.73
		B	338.71	8.16	47.64
		C	342.85	15.11	149.51
		D	351.12	16.80	304.27
	Ethanol	A	356.72	9.61	54.42
		B	358.71	13.03	100.21
		C	360.95	27.74	276.51
		D	362.96	32.93	369.50

Foam thickness	Fluid	Case	T_w [K]	h_{exp} [kW/m^2·K]	q'' [kW/m^2]
1 mm	HFE-7100	A	339.99	2.81	19.57
		B	340.05	6.57	46.15
		C	343.37	13.86	145.00
		D	348.47	18.94	293.96
	Ethanol	A	358.85	7.01	53.63
		B	358.99	13.02	104.01
		C	360.78	24.27	237.52
		D	362.56	32.82	379.65

[a]$T_{\infty,HFE-7100}$ = 333.3 K; [b]$T_{\infty,Ethanol}$ = 351.1 K.

3. DATA ANALYSIS

With the results of the numerical experiments, we calculated the heat transfer rate from the solid to the fluid, q_{foam}, as follows:

$$q_{foam} = \int_{A_{foam}} h_{exp}[T(x) - T_\infty]dA_{foam}, \quad (1)$$

where A_{foam} is the foam wetted area (convective area) and T_∞ is the working fluid temperature at saturation conditions. The result from Eq. (1) allow us to calculate the foam efficiency, η_{foam},

$$\eta_{foam} = \frac{q_{foam}}{q_{max}}, \quad (2)$$

where the maximum heat transfer rate, q_{max}, is obtained by:

$$q_{max} = (T_w - T_\infty)A_{foam}h_{exp} \quad (3)$$

corresponding to the heat transfer rate at ideal conditions.

The foam efficiency calculated as indicated above was compared with selected analytical models from the literature (three classical ones presented in a heat transfer technical book (Bergman and Incropera, 2011)), consisting of a circular pin fin of uniform cross-section and one-dimensional heat transfer. As Dukhan et al. (2005), the metal foams were simplified as a bank of one-dimensional circular cylinders, which diameter was equal to the foam fiber diameter, d_f.

The first classical analytical model used for comparison was the well-known model of the fin with an adiabatic tip. The foam-finned efficiency can be calculated by using:

$$\eta_{foam,pin-fin-1} = \frac{q_{pin-fin-1}}{q_{max}} = \frac{\tanh(mL)}{mL} \quad (4)$$

where

$$m^2 = \frac{h_{exp}P}{k_s A_c} = \frac{4h_{exp}}{k_s d_f} \quad (5)$$

where P is the foam fiber perimeter, A_c is the foam fiber cross-section area, k_s is the thermal conductivity from the foam fiber (solid phase), and L is the thickness of the foam.

The second classical analytical model was the fin with convection heat transfer on the tip in which the foam-finned efficiency can be calculated as follows:

$$\eta_{foam,pin-fin-2} = \frac{q_{pin-fin-2}}{q_{max}} \quad (6)$$

where

$$q_{pin-fin-2} = M\frac{\sinh mL + \left(\frac{h}{mk}\right)\cosh mL}{\cosh mL + \left(\frac{h}{mk}\right)\sinh mL} \quad (7)$$

and

$$M = \sqrt{h_{exp} P A_c}(T_w - T_\infty). \tag{8}$$

Finally, the third classical analytical model was the infinite fin with foam-finned efficiency calculated as:

$$\eta_{foam,pin-fin-3} = \frac{q_{pin-fin-3}}{q_{max}} = \frac{M}{q_{max}} \tag{9}$$

where the maximum heat transfer rate, q_{max}, for the last two models is calculated as:

$$q_{max} = h_{exp} A_{pin-fin}(T_w - T_\infty). \tag{10}$$

where $A_{pin-fin}$ is the convective area from one metal foam fiber (considering a cylinder with the fiber diameter).

In addition, the results were also compared with specific models for open-cell foams. The first specific model was from Ghosh (2008), based on the traditional fin theory. The model considers the random geometry of the solid ligaments as a repetitive cubic structure. The authors calculated the foam efficiency as follows:

$$\eta_{foam,Ghosh} = \frac{\tanh ML}{ML} \tag{11}$$

where,

$$M = \sqrt{\frac{h_{exp} P}{k_s A_c}\left(1 + 4\eta_{1/2}\right)} = m\sqrt{1 + 4\eta_{1/2}} \tag{12}$$

where $\eta_{1/2}$ is the efficiency of the half fiber in the perpendicular direction of the thickness due to cross-connections in the foam filaments, given by:

$$\eta_{1/2} = \frac{tanh\left(m\, d_p/2\right)}{\left(m\, d_p/2\right)} \tag{13}$$

The two last models were obtained from Mancin et al. (2013, 2010), who developed a simplified scheme for overall foam-finned surface efficiency which takes into account the foam surface area density (a_{sf}),

$$\eta_{foam,Mancin} = \frac{1 + \Omega \cdot a_{sf} \cdot L}{1 + a_{sf} \cdot L} \tag{14}$$

where

$$\Omega = \frac{\tanh\left(m_{eq} \cdot L_{eq}\right)}{\left(m_{eq} \cdot L_{eq}\right)} \tag{15}$$

where m_{eq} and L_{eq} (equivalent thickness) were adjusted to experimental data yielding:

- Mancin et al. (2010),

$$m_{eq} = \sqrt{\frac{4h_{exp}}{k_s d_f}} \tag{16}$$

$$L_{eq} = 6.6 \cdot L \cdot \mathrm{PPI}^{0.99}\left(0.0254 - d_f \cdot \mathrm{PPI}\right) \tag{17}$$

- Mancin et al. (2013),

$$m_{eq} = \sqrt{\frac{4h_{exp}}{k_s d_f}}\left(\frac{k_s}{k_l}\right)^{-0.52} \tag{18}$$

$$L_{eq} = 1055 \cdot L^{1.18} \cdot \mathrm{PPI}\left(0.0254 - d_f \cdot \mathrm{PPI}\right)^{0.66} \tag{19}$$

where k_l is the liquid (working fluid) thermal conductivity.

4. RESULTS AND DISCUSSION

In general, for all surfaces-fluid combinations, the first case of BCs, *i.e.*, case A relative to the low heat flux, presents the best foam-finned efficiency, as shown in Table 3. According to the experimental work of Manetti et al. (2020a), at low heat flux, there are just a few bubbles on the surface, which cause a lower HTC and the temperature field is more uniform in the foam. Hence the foam heat transfer rate, q_{foam}, is close to the maximum heat transfer rate, q_{max}. As the experimental heat flux increases, the wall temperature (foam base) and HTC also increase. On the other hand, the foam-finned efficiency decreases because the higher HTC dissipates the heat faster, and therefore, there is no need to use the entire foam thickness. Moreover, as the thickness decreases, the foam-finned efficiency increases; so, the thicker foams have a significant part of their length useless. Therefore, there is a balance between thickness, efficiency, and heat transfer rate.

Table 3. Heat transfer rate through the foam surface and maximum heat transfer rate from the numerical simulation results.

Foam thickness	Fluid	Case	q_{foam} [W]	q_{max} [W]	η_{foam} [-]
3 mm[a]	HFE-7100	A	1.08	1.97	0.55
		B	2.08	4.42	0.47
		C	5.43	14.10	0.39
		D	10.53	28.47	0.37
	Ethanol	A	2.26	5.44	0.42
		B	3.47	10.09	0.34
		C	6.37	23.61	0.27
		D	9.12	35.53	0.26
2 mm[b]	HFE-7100	A	1.00	1.55	0.64
		B	1.95	3.56	0.55
		C	4.77	11.18	0.43
		D	9.29	22.76	0.41
	Ethanol	A	2.08	4.07	0.51
		B	3.41	7.50	0.45
		C	6.77	20.69	0.33
		D	8.39	27.64	0.30
1 mm[c]	HFE-7100	A	0.64	0.69	0.93
		B	1.39	1.63	0.85
		C	3.81	5.13	0.74
		D	7.18	10.40	0.69
	Ethanol	A	1.60	1.90	0.84
		B	2.77	3.68	0.75
		C	5.42	8.40	0.65
		D	7.91	13.43	0.59

[a]$A_{3\mathrm{mm}}$ = 96.56 mm^2; [b]$A_{2\mathrm{mm}}$ = 74.81 mm^2; [c]$A_{1\mathrm{mm}}$ = 35.38 mm^2

Figure 3a and Figure 3b present the foam efficiency *vs.* the experimental heat flux for the three foams thicknesses and both fluids, HFE-7100 and Ethanol, respectively. One may observe that Cu foam 3 mm and Cu foam 2 mm have the worst performance of Cu foam 1 mm for the four BCs analyzed. There is a slight difference in the foam-finned efficiency from 3 mm to 2 mm; however, there is a significant difference from 2 mm to 1 mm. So, the temperature field for 3 mm and 2 mm is quite the same, while Cu foam 1 mm is close to the wall temperature for the entire length.

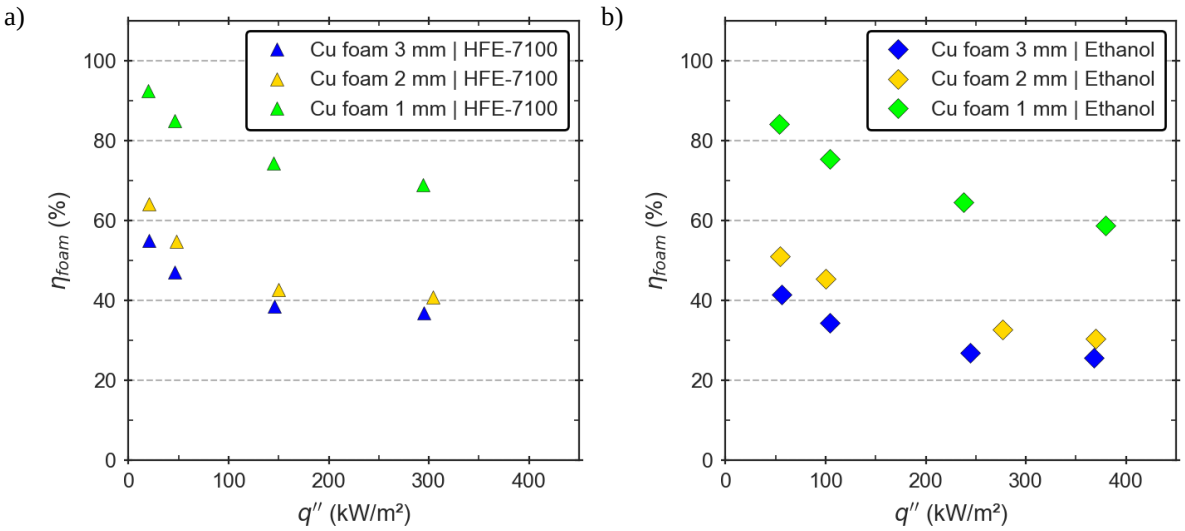

Figure 3. Foam efficiency as a function of experimental heat flux for different foam thicknesses and (a) HFE-7100 and (b) Ethanol.

Figure 4 and Figure 5 present the temperature fields of the numerical results of the extreme cases (A and D) for all three foams thicknesses and both fluids, HFE-7100 and Ethanol, respectively. The Cu foam of 1 mm presents a temperature field relatively uniform, mainly for Case A, while 2 mm and 3 mm present a temperature gradient.

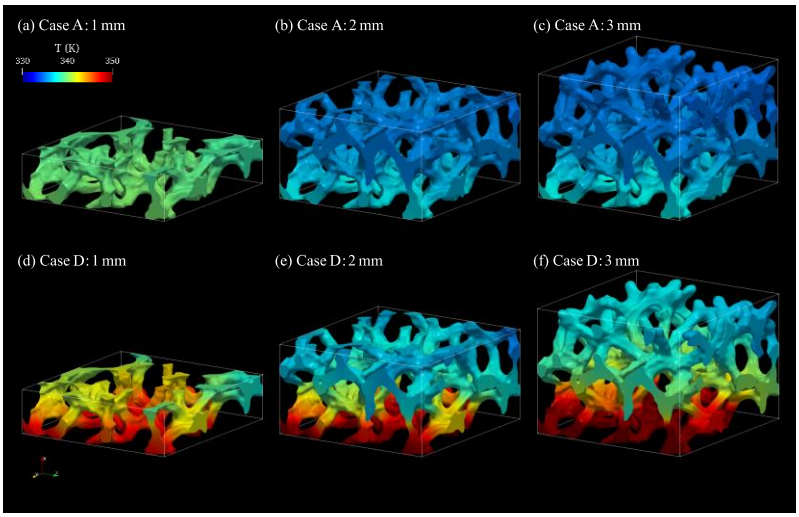

Figure 4. Temperature distribution in the Cu foam with different thicknesses and Cases A and D (Table 3) for HFE-7100.

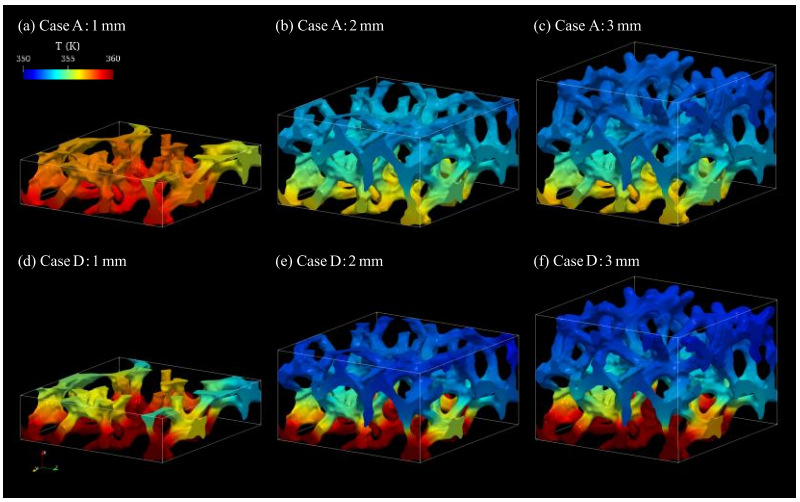

Figure 5. Temperature distribution in the Cu foam with different thicknesses and Cases A and D (Table 3) for Ethanol.

Figure 6, Figure 7 and 8 compare the numerical results and the efficiency models presented in Section 4. The mean absolute percentual error (MAPE) for each analytical model relative to the numerical data is shown in each plot. For all foams, the classical models (circular pin fin models) presented lower error than the specific models; comparing the adiabatic tip and convection tip for all thicknesses, the pin fin model with an adiabatic tip is the best one to predict the numerical results with the lowest MAPE (lower than 10% for all cases). In addition, the Cu foam 3 mm with HFE-7100 is the case with the lowest error, approximately 1%, probably due to the convection area, which is more significant in the radial area (lateral) than in the axial area (tip). The specific models presented more significant error probably due to the modeling conditions used in Mancin et al. (2013, 2010), which use empirical factors from experimental tests with forced air convection. Ghosh's model (2008) presents a similar trend as the 1D circular pin fin; however, the values are two times smaller. The lowest efficiency presented by Ghosh's model should be the term $\eta_{1/2}$ related to the cross-connection in the simple cubic structure. Therefore, the one-dimensional pin fin model provides efficiencies closer to the numerical simulation results for the boiling process.

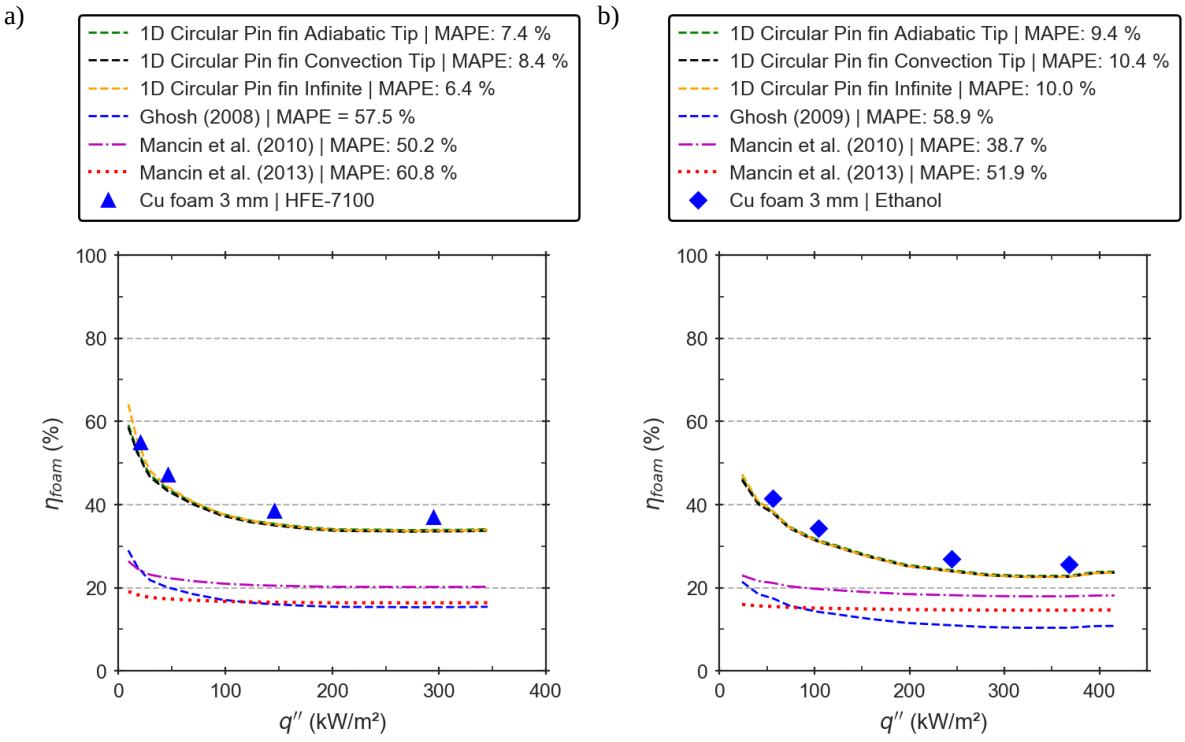

Figure 6. Comparison for foam efficiency between numerical results and analytical models, for Cu foam 3 mm and boiling of (a) HFE-7100 and (b) Ethanol.

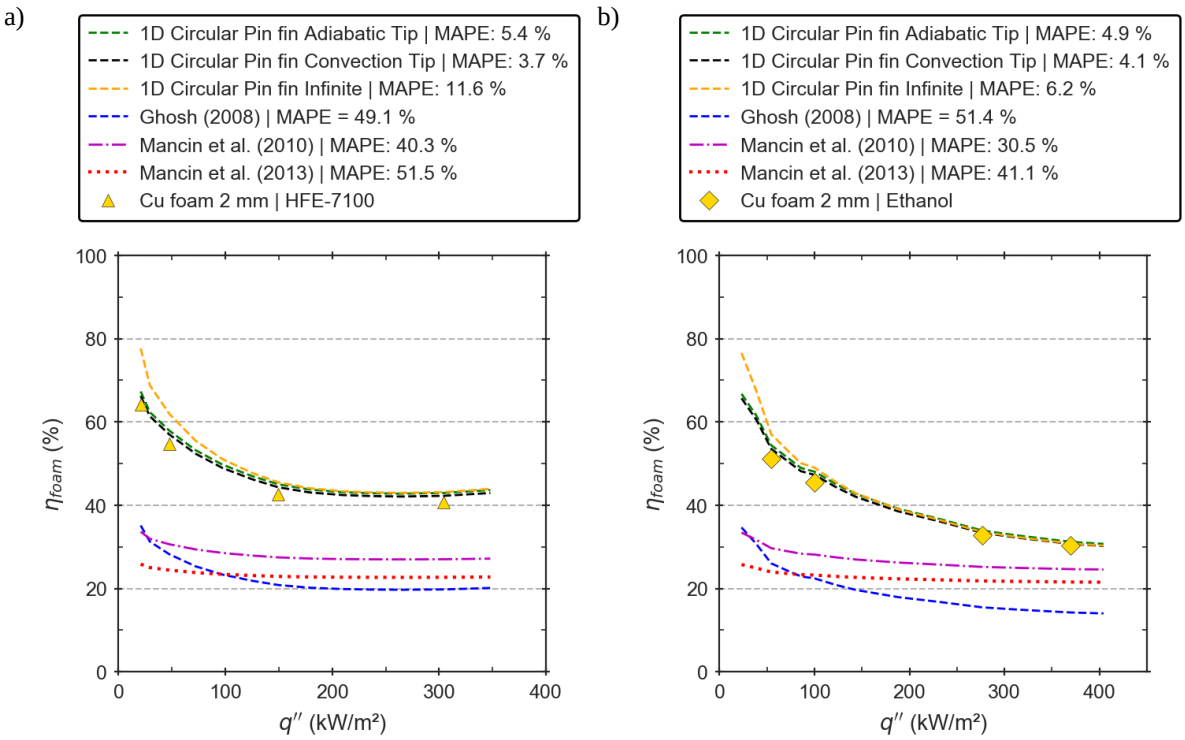

Figure 7. Comparison for foam efficiency between numerical results and analytical models, for Cu foam 2 mm and boiling of (a) HFE-7100 and (b) Ethanol.

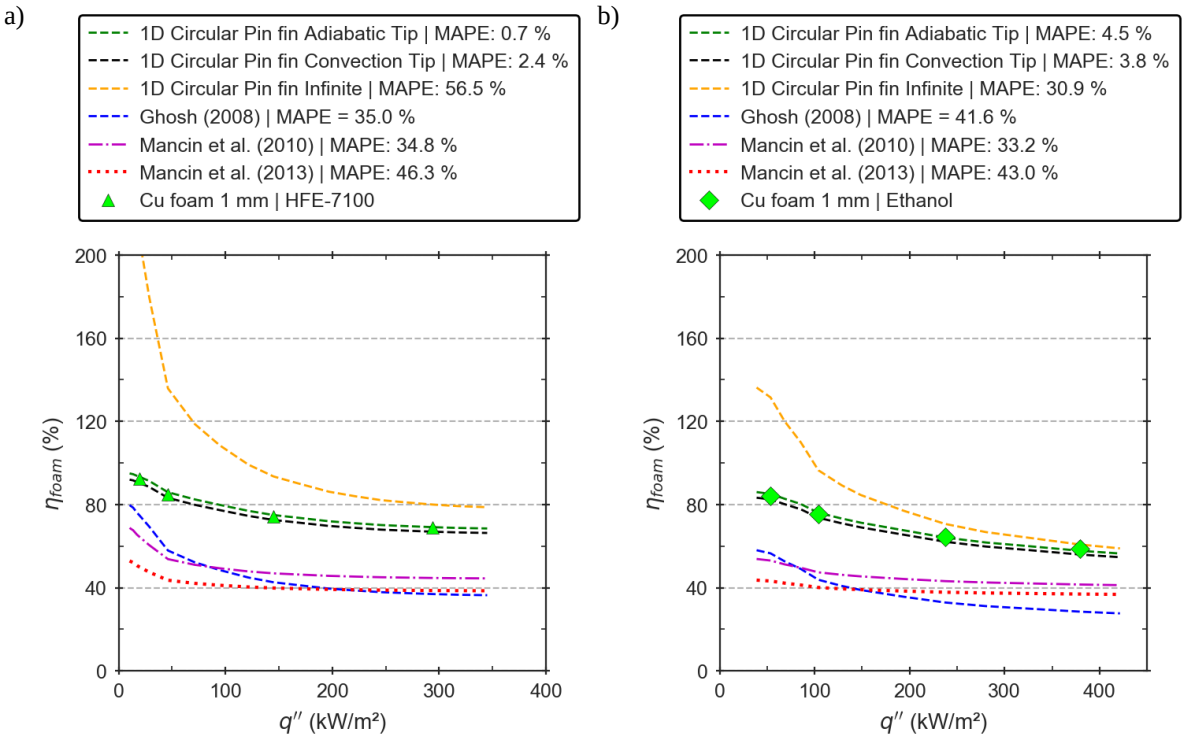

Figure 8. Comparison for foam efficiency between numerical results and analytical models, for Cu foam 13 mm and boiling of (a) HFE-7100 and (b) Ethanol.

5. CONCLUSION

This paper presented a heat transfer numerical study using foam-extend and BCs based on experimental data obtained by pool boiling of dielectric fluids on copper metal foams to calculate the foam-finned efficiency. Besides, the

numerical data were compared with foam-finned efficiency models available in the literature. As a result, the following conclusions can be drawn:

- ✓ The numerical data represent well the findings of previous works, in which the foam-finned efficiency increases as the thickness decreases; and the foam-finned efficiency decreases as the heat flux increases;
- ✓ The thinnest the foam, the highest the foam-finned efficiency for all cases; thus, the temperature field in the thinnest foam is close to the wall temperature. Besides, pool boiling using HFE-7100 as the working fluid has higher efficiency than pool boiling using Ethanol due to the lowest heat transfer coefficient for HFE-7100.
- ✓ The classical pin fin model with an adiabatic tip has the lowest MAPE compared to the numerical data, lower than 10% for all cases.

6. ACKNOWLEDGEMENTS

This research was supported by resources supplied by the Center for Scientific Computing (NCC/GridUNESP) of the São Paulo State University (UNESP) (www2.unesp.br/portal#!/gridunesp). In addition, the authors are grateful for the financial support from CAPES and FAPESP (grants number 2013/15431-7, 2019/02566-8, 2017/13813-0, 2019/15250-9). We also extend our gratitude to Prof. Dr. Alessandro R. Rodrigues, Prof. Dr. Tito J. Bonagamba (EESC-USP), and Prof. Dr. Ana Moita (IST/Lisbon) for their important contribution to this work.

7. REFERENCES

Al-Athel, K.S., 2017. "A computational methodology for assessing the thermal behavior of metal foam heat sinks". *Applied Thermal Engineering*, Vol. 111, pp. 884–893.

Bergman, T.L., Incropera, F.P., 2011. *Fundamentals of heat and mass transfer*, 7th ed. ed. Wiley, Hoboken, NJ.

Chen, P., Harmand, S., Ouenzerfi, S., 2020. "Immersion cooling effect of dielectric liquid and self-rewetting fluid on smooth and porous surface". *Applied Thermal Engineering*, Vol. 180, pp.115862.

Dukhan, N., Quiñones-Ramos, P.D., Cruz-Ruiz, E., Vélez-Reyes, M., Scott, E.P., 2005. "One-dimensional heat transfer analysis in open-cell 10-ppi metal foam". *International Journal of Heat and Mass Transfer*, Vol. 48, pp. 5112–5120.

El-Genk, M.S., 2012. "Nucleate boiling enhancements on porous graphite and microporous and macro-finned copper surfaces". *Heat Transfer Engineering*, Vol. 33, pp. 175–204.

Fan, S., Duan, F., 2020. "A review of two-phase submerged boiling in thermal management of electronic cooling". *International Journal of Heat and Mass Transfer*, Vol. 150, pp. 119324.

Ghosh, I., 2008. "Heat-transfer analysis of high porosity open-cell metal foam". *Journal of heat transfer*, Vol. 130.

Jasak, H., 1996. *Error analysis and estimation for the finite volume method with applications to fluid flows*.

Kiyomura, I.S., Nunes, J.M., de Souza, R.R., Gajghate, S.S., Bhaumik, S., Cardoso, E.M., 2020. "Effect of microfin surfaces on boiling heat transfer using HFE-7100 as working fluid". *J Braz. Soc. Mech. Sci. Eng.*, Vol. 42, pp. 366.

Liang, G., Mudawar, I., 2019. "Review of pool boiling enhancement by surface modification". *International Journal of Heat and Mass Transfer*, Vol. 128, 892–933.

Mancin, S., Zilio, C., Cavallini, A., Rossetto, L., 2010. "Heat transfer during air flow in aluminum foams". *International Journal of Heat and Mass Transfer*, Vol. 53, pp. 4976–4984.

Mancin, S., Zilio, C., Diani, A., Rossetto, L., 2013. "Air forced convection through metal foams: Experimental results and modeling". *International Journal of Heat and Mass Transfer*, Vol. 62, pp. 112–123. https://doi.org/10.1016/j.ijheatmasstransfer.2013.02.050

Manetti, L.L., Moita, A.S.O.H., Cardoso, E.M., 2021. "A new pool boiling heat transfer correlation for wetting dielectric fluids on metal foams". *International Journal of Heat and Mass Transfer*, Vol. 171, pp. 121070. https://doi.org/10.1016/j.ijheatmasstransfer.2021.121070

Manetti, L.L., Moita, A.S.O.H., de Souza, R.R., Cardoso, E.M., 2020b. "Effect of copper foam thickness on pool boiling heat transfer of HFE-7100". *International Journal of Heat and Mass Transfer*, Vol. 152, pp. 119547.

Manetti, L.L., Ribatski, G., de Souza, R.R., Cardoso, E.M., 2020a. "Pool boiling heat transfer of HFE-7100 on metal foams". *Experimental Thermal and Fluid Science*, Vol. 113, pp. 110025.

8. RESPONSIBILITY NOTICE

The authors are the only ones responsible for the printed material included in this paper.